



# A novel homozygous missense mutation in the SH3-binding motif of *STAMBP* causing microcephaly-capillary malformation syndrome

Ikumi Hori<sup>1</sup> · Fuyuki Miya<sup>2,3</sup> · Yutaka Negishi<sup>1</sup> · Ayako Hattori<sup>1</sup> · Naoki Ando<sup>1</sup> · Keith A. Boroevich<sup>3</sup> · Nobuhiko Okamoto<sup>4</sup> · Mitsuhiro Kato<sup>5</sup> · Tatsuhiko Tsunoda<sup>2,3</sup> · Mami Yamasaki<sup>6</sup> · Yonehiro Kanemura<sup>7,8</sup> · Kenjiro Kosaki<sup>9</sup> · Shinji Saitoh<sup>1</sup>

Received: 19 February 2018 / Revised: 4 June 2018 / Accepted: 4 June 2018 / Published online: 15 June 2018  
© The Author(s) under exclusive licence to The Japan Society of Human Genetics 2018

## Abstract

Microcephaly-capillary malformation syndrome is a congenital and neurodevelopmental disorder caused by biallelic mutations in the *STAMBP* gene. Here we identify the novel homozygous mutation located in the SH3 binding motif of *STAMBP* (NM\_006463.4) (c.707C>T: p.Ser236Phe) through whole-exome sequencing. The case patient was a 2-year-old boy showing severe global developmental delay, progressive microcephaly, refractory seizures, dysmorphic facial features, and multiple capillary malformations. Immunoblot analysis of patient-derived lymphoblastoid cell lines (LCLs) revealed a severe reduction in *STAMBP* expression, indicating that Ser236Phe induces protein instability. *STAMBP* interacts with the SH3 domain of *STAM* and transduces downstream signals from the Jaks-*STAM* complex. The substitution of Ser236Phe found in the case patient was located in the SH3-binding motif, and we propose the mutation may block *STAM* binding and subsequently induce *STAMBP* degradation. Contrary to previously reported *STAMBP* mutations, the Ser236Phe mutation did not lead to constitutive activation of the PI3K-AKT-mTOR pathway in patient-derived LCLs, as indicated by the expression of phosphorylated S6 ribosomal protein, suggesting that it is not the major pathomechanism underlying the disorder in this patient.

## Introduction

Biallelic mutations in the *STAM-binding protein* gene (*STAMBP*, alias *associated molecule with the SH3 domain*

*of STAM*, *AMSH*) on chromosome 2p13 cause microcephaly-capillary malformation syndrome (MICCAP: OMIM #614261) [1]. Patients with MICCAP show severe progressive microcephaly, profound intellectual disability, early-onset intractable epilepsy, and generalized capillary malformations on the skin. Dysmorphic facies, distal limb abnormalities, and congenital heart diseases are also often associated with the syndrome [2, 3]. Clinical features are summarized in Table 1. One patient had mild phenotype [4]. Her birth occipitofrontal circumference (OFC) was normal.

These authors contributed equally: Ikumi Hori, Fuyuki Miya

**Electronic supplementary material** The online version of this article (<https://doi.org/10.1038/s10038-018-0482-3>) contains supplementary material, which is available to authorized users.

✉ Shinji Saitoh  
ss11@med.nagoya-cu.ac.jp

- 1 Department of Pediatrics and Neonatology, Nagoya City University Graduate School of Medical Sciences, Nagoya, Japan
- 2 Medical Research Institute, Tokyo Medical and Dental University, Tokyo, Japan
- 3 Laboratory for Medical Science Mathematics, RIKEN Center for Integrative Medical Sciences, Yokohama, Japan
- 4 Department of Medical Genetics, Osaka Women's and Children's Hospital, Osaka, Japan

- 5 Department of Pediatrics, Showa University School of Medicine, Tokyo, Japan
- 6 Department of Neurosurgery, Takatsuki General Hospital, Osaka, Japan
- 7 Division of Regenerative Medicine, Institute for Clinical Research, Osaka National Hospital, National Hospital Organization, Osaka, Japan
- 8 Department of Neurosurgery, Osaka National Hospital, National Hospital Organization, Osaka, Japan
- 9 Center for Medical Genetics, Keio University School of Medicine, Tokyo, Japan

**Table 1** Clinical features of our patient and previously reported patients

Clinical feature	Our patient	Previously reported 16 patients with <i>STAMBP</i> mutations <sup>1, 5–7</sup>
Sex	Male	12 males, 4 females
Congenital microcephaly	+	15/16 (94%)
Progressive microcephaly	+	12/16 (75%)
Capillary malformations of the skin	+	16/16 (100%)
Hypoplastic distal phalanges	–	16/16 (100%)
Hypertelorism	+	9/9 (100%)
Severe developmental delay	+	15/16 (94%)
Seizures		
Infantile onset	+	15/16 (94%)
Intractable	+	15/16 (94%)
Growth retardation	–	9/11 (82%)
Spasticity	–	12/16 (75%)
Optic atrophy	–	12/14 (86%)

She had controllable epilepsy and moderate developmental delay. *STAMBP* encodes a deubiquitinating (DUB) isopeptidase that is important for cell surface receptor-mediated endocytosis and sorting [1]. Previously 16 patients with *STAMBP* mutations were reported. The identified mutations included seven missense, two nonsense, two frameshift, and five splicing mutations [1, 5–7]. Previously it was reported that the insensitive activation of RAS-mitogen activated protein kinase (RAS-MAPK) and phosphatidylinositol-3-kinase (PI3K)-AKT-mammalian target of rapamycin (mTOR) pathways might contribute to vascular and capillary malformation and apoptosis induction by a defective DUB might be responsible for microcephaly [1]. Here we present a patient with microcephaly, severe developmental delay, and intractable epilepsy carrying a novel homozygous mutation located in the SH3-binding motif of *STAMBP*.

## Materials and methods

### Case presentation

We report a 2-year-old boy with no family history of any relevant diseases and a healthy older sister. The clinical features of our patient are summarized in Table 1. The boy was born by vaginal delivery at 37 gestational weeks from Japanese parents. To examine the relatedness, we calculated estimate value of relatedness between individuals.

His parents were assumed not to be consanguineous (Supplementary Figure). He had no perinatal abnormalities and his newborn screening was normal. His birth weight was 2680 g (−0.8 SD), length was 48.0 cm (−0.5 SD), and head circumference was 33.0 cm (0 SD). The social smile appeared around 2 months of age. He presented to our hospital at 6 months of age when he could not hold up his head. At this age, he was not able to visually track an object, and physical examination found that his weight was 7.4 kg (−0.7 SD), and head circumference was 41.6 cm (−1.3 SD). There were multiple capillary malformations on the trunk and extremities, ranging from 2 to 15 mm in size (Fig. 1b, c). When he was evaluated at 2 years and 4 months of age, he had a weight of 10.15 kg (−1.7 SD), length of 87.5 cm (−0.3 SD), and OFC of 43.4 cm (−3.5 SD). He was still unable to hold up his head, neither spoke meaningful words nor targeted visual tracking, and had no social interactions, indicating severe developmental delay. Dysmorphic features included hypertelorism, ptosis, and downturned mouth (Fig. 1a). He had no hypoplastic distal phalanges. When he had a viral infection, his feeding became poor that sometimes necessitated tube feeding. At 7 months, he developed seizures. Electroencephalogram showed frequent spikes in the occipital region with diffusely slow background. Focal onset seizures with turning of his eyes to one side, with excessive salivation and drooling, impaired awareness, and cyanosis occurred more than three times per hour. Seizures were refractory to many antiepileptic drugs, requiring hospitalization for several months.

Karyotype and chromosome microarray revealed normal results, as was metabolic screening, including plasma lactic acid and pyruvic acid. A brain magnetic resonance imaging was performed at age 1 and 3 years. It showed symmetric cerebral atrophy and progressive cerebellar atrophy (Fig. 2). Ophthalmologic exam, echocardiography, auditory brainstem response, and nerve conduction studies showed normal results. In a somatosensory evoked potential study, N20 was not detected, suggesting dysfunction of somatosensory pathways.

## Methods

### Whole-exome sequencing

We performed whole-exome sequencing on the proband and parents. Genomic DNA was captured using the SureSelect XT Human All Exon V5 capture library (Agilent Technologies, Santa Clara, CA, USA) and sequenced using the Illumina HiSeq 2000 (Illumina, San Diego, CA, USA) with 100 bp paired-end reads. Exome data processing, variant calling, and variant annotation were performed as described previously [8]. The ClinVar accession numbers

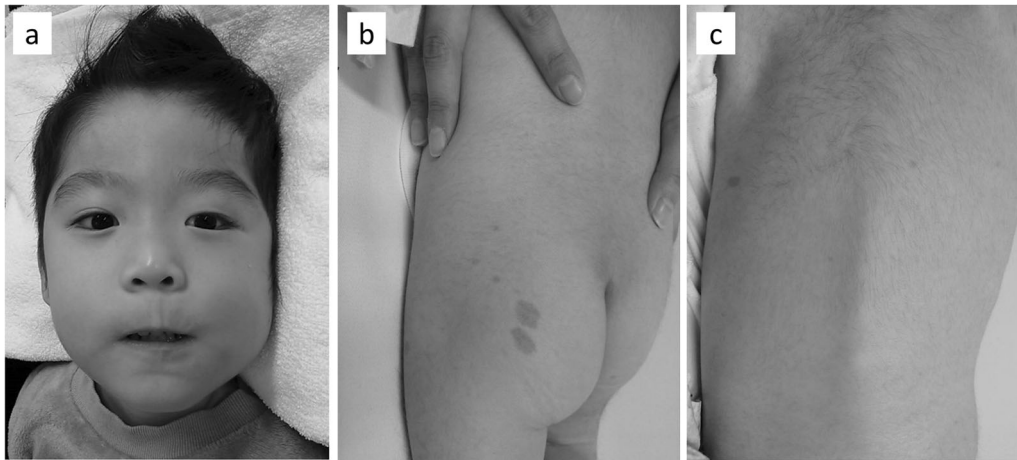


**Fig. 1** Case presentation. **a–c** Representative photographs of the patient showing dysmorphic features, including hypertelorism, ptosis, and downturned mouth **a**, and multiple capillary malformations **b**, **c**. His parents gave informed consent for publication of this image

for the DNA variants reported in this paper are SCV000676941 (ClinVar, <https://www.ncbi.nlm.nih.gov/clinvar/>). Genetic relatedness between parents was calculated by PLINK PI\_HAT statistics [9]. Expected values of PI\_HAT are 0.5 for first-degree relatives and 0.25 for second-degree relatives.

#### Cell culturing and western blotting

Patient-derived Epstein–Barr virus-transformed lymphoblastoid cell lines (LCLs) and control wild-type (WT) LCLs derived from two different healthy individuals were grown at 5% CO<sub>2</sub> in complete medium in the presence of 10% fetal bovine serum (FBS) or starved conditions (0.1% FBS and no FBS) for 2, 4, and 24 h. Equal amounts of protein were boiled with sodium dodecyl sulfate (SDS) sample buffer (45 mmol/L Tris-HCl, pH 6.8, 10% glycerol, 1% SDS, 0.01% bromophenol blue, 50 mmol/L DTT). Proteins in the lysates were separated by SDS-polyacrylamide gel electrophoresis and transferred to polyvinylidene difluoride membranes (Millipore, Billerica, MA, Japan). Membranes were blocked for 1 h with 5% dried skimmed milk in phosphate-buffered saline with 0.1% Tween-20 (Sigma-Aldrich). Membranes were then incubated overnight with primary antibodies against phosphorylated S6 ribosomal protein (pS6) (Ser240/244; #5018; diluted 1:1000; Cell Signaling Technology, Danvers, MA, USA), and glyceraldehyde 3-phosphate dehydrogenase (diluted 1:10,000; Cell Signaling Technology), followed by 1 h incubation with horseradish peroxidase-conjugated secondary antibody (GE Healthcare, Little Chalfont, UK). *STAMBP* expression in the LCLs was assessed by protein blotting using an anti-*STAMBP* antibody (#5245; diluted 1:1000; Cell Signaling Technology, Danvers, MA, USA).

#### Statistical analysis

Data were analyzed with a two-tailed Student's *t* test.

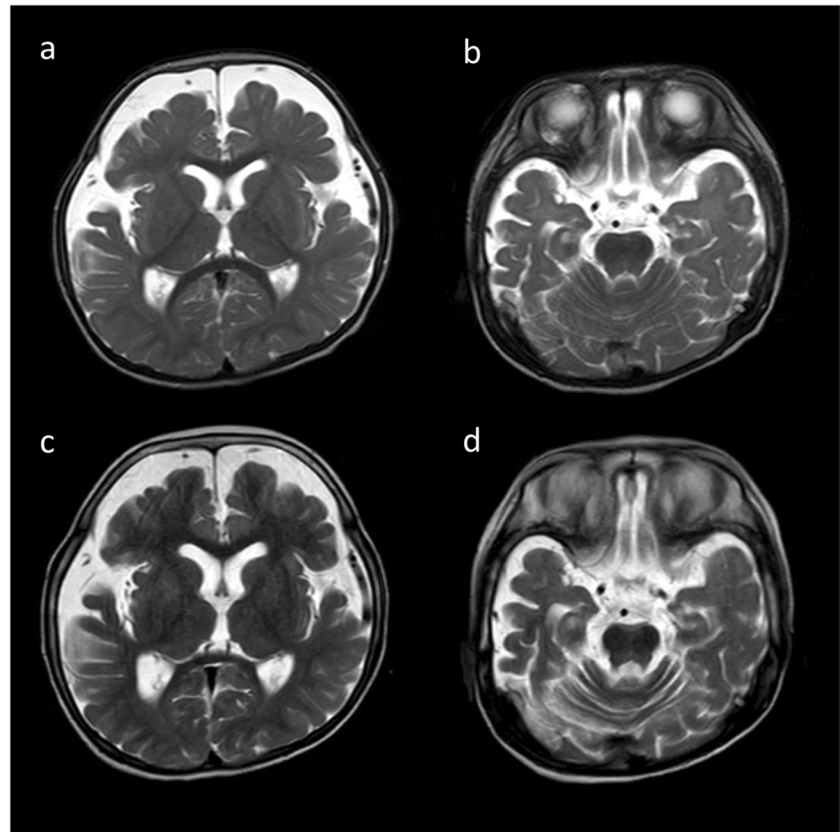
This research was approved by the Ethical Committee of Nagoya City University Graduate School of Medical Sciences (#213), and written informed consent was obtained from the patient's parents.

## Results

#### Mutation analysis of case patient and parents

Whole-exome sequencing of the patient identified a homozygous mutation in the *STAMBP* gene (NM\_006463.4) (c.707C>T: p.Ser236Phe). Sanger sequencing confirmed that the parents were heterozygous for the same mutation (Fig. 3a). The mutation is located in the SH3-binding motif that interacts with the SH3 domain of STAM (Fig. 3b). The mutation was predicted to be damaging by SIFT (score 0.003), PolyPhen-2 (HDIV score 0.748), and MutationTaster (probability value 0.999). The raw CADD score was 6.85 and scaled *C*-score was 33, indicating pathogenicity. The mutation was not registered in the 1000 Genomes Project, Exome Sequencing Project 6500, Human Genetic Variation Database, Human Genetic Mutation Database (ver2017.3), UK10K, and ClinVar databases as of December 2017. Only 3 of the 60,543 individuals (minor allele frequency (MAF) = 0.00005) and 1 of the 3545 individuals (MAF = 0.00028) were heterozygous carriers of the mutation in the Exome Aggregation Consortium and the Integrative Japanese Genome Variation (3.5 K Japanese) databases, respectively. No homozygous carriers of the mutation have been registered in any database.

**Fig. 2** Brain MRI scans of the patient. Representative T2-weighted axial images at age 1 year and 1 month **a, b** and at age 3 years and 2 months **c, d**



Two additional homozygous mutations were found in the patient: in *EFHB* (NM\_144715: c.268G>A: p.Gly90Arg) and *SATL1* (NM\_001012980: c.1774G>A: p.Gly592Ser). In addition, we discovered two de novo heterozygous nonsynonymous mutations (*OBSCN* [NM\_001271223: c.2513G>A: p.Gly838Asp], *TBX3* [NM\_005996: c.1153C>A: p.Arg385Ser]) and three compound heterozygous nonsynonymous mutations (*ANO5* [NM\_001142649: c.581G>A: p.Arg194Gln and c.2700T>G: p.Ile900Met], *C16orf90* [NM\_001080524: c.444G>C: p.Gln148His and c.172C>T: p.Arg58Trp], and *C2orf16* [NM\_032266: c.1940C>T: p.Ala647Val and c.4928\_4951del: p.Arg1645\_Arg1652del]). It is unlikely that these variants are pathogenic as the patient did not clinically fit the phenotype, and therefore Sanger sequencing validation was not performed.

### Analysis of PI3K–AKT–mTOR pathway function and STAMBP expression

To investigate PI3K, AKT, and mTOR signaling pathway function in the patient, we analyzed patient-derived Epstein–Barr virus-transformed LCLs for the expression of phosphorylated S6 protein levels. Serum starvation of LCLs significantly reduced the expression of pS6 protein in both WT and patient-derived LCLs (Fig. 4a, b), indicating

that the patient-derived LCLs did not have independent activation of PI3K–AKT–mTOR pathway. We initially performed the assay in the manner described by McDonnell et al. [1], specifically serum-starving the cells with no FBS for 24 h. However, at 24 h most cells were non-viable, and as such we could not assess pS6 levels. For this reason, we instead assessed pS6 levels following 2 and 4 h of serum starvation with 0.1% FBS.

Protein expression analysis of patient-derived LCLs revealed a marked reduction in *STAMBP* expression compared with WT LCLs (Fig. 4c). *STAMBP* expression in patient's mother, who had a heterozygous mutation in the *STAMBP* gene, was mildly reduced compared with WT LCLs (Fig. 4c).

### Discussion

Here we are the first to report a mutation in the SH3-binding motif (Pro231 to Pro239) of the *STAMBP* gene. *STAMBP* is a member of the JAB1/MPN/Mov34 metalloenzyme (JAMM) family of DUBs. *STAMBP* contains a microtubule-interacting and transport domain and an SH3-binding motif, both of which regulate the endosomal sorting and trafficking machinery [10]. *STAMBP* interacts with the SH3 domain of STAM through the SH3-binding motif and

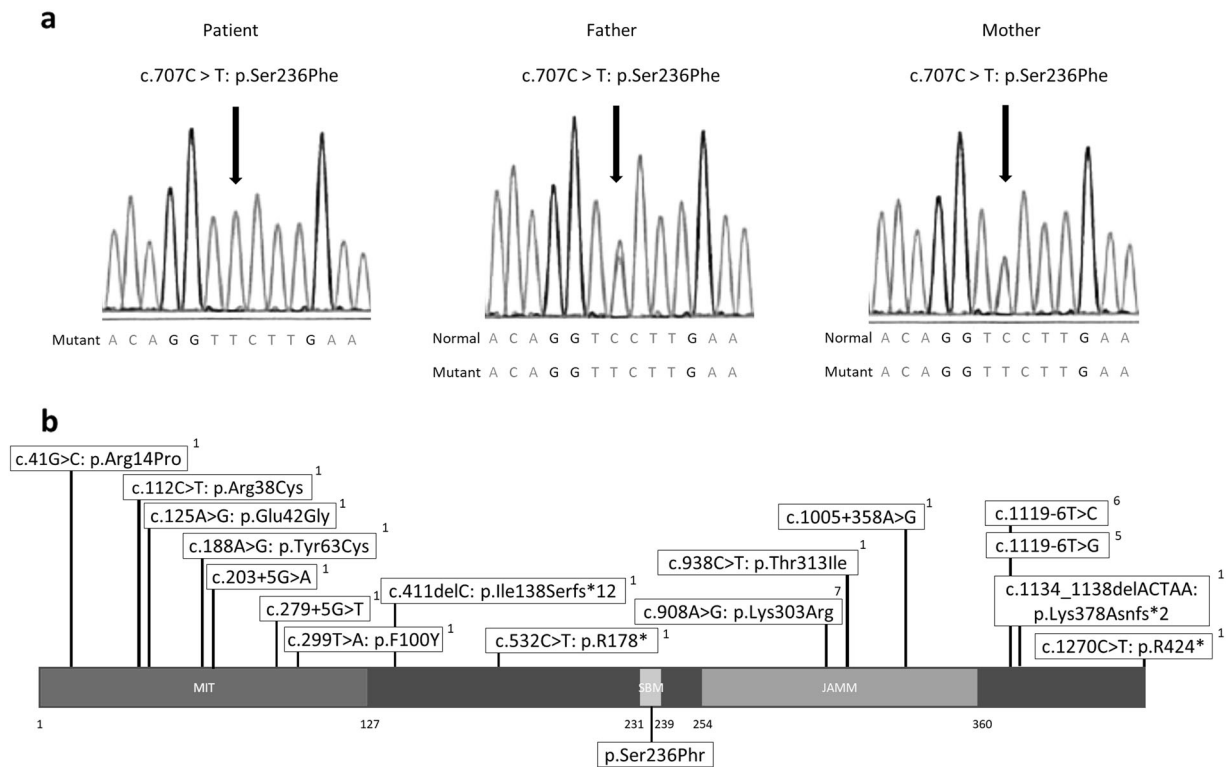


**Fig. 3** Detection and location of *STAMBP* mutation in case patient. **a** Sanger sequencing of the *STAMBP* mutation showed that the case patient has a homozygous mutation c.707C>T: p.Ser236Phe (arrow) while the parents have a heterozygous mutation. **b** Schematic representation of the structure of *STAMBP*. Known mutations in *STAMBP*

are shown above the protein and the novel mutation identified in the case patient is shown below the protein. We described reference number on the upper right of the mutation. *STAMBP* contains an MIT domain, an SH3-binding motif (SBM) (PX [V/I] [D/N] RXXP), and a JAMM (JAB1/MPN/MOV34) motif

plays an important role in downstream signaling from the Jaks-STAM complex [11]. As the Ser236Phe substitution found in the case patient is located in the SH3-binding motif, the mutation may interfere with *STAMBP* interacting with *STAM* and consequently downstream signaling.

Analysis of protein expression found decreased levels of the mutant *STAMBP*, with the homozygous mutant exhibiting a larger decrease in expression than the heterozygous mutant. This indicates the Ser236Phe mutation induces protein instability with the total amount of *STAMBP* significantly reduced in the homozygous mutant patient. McDonnell et al. [1] reported decreased expression of *STAMBP* in some MICCAP patients, and *STAMBP*-deficient mice showed significant neuron loss and apoptotic cells, developing brain atrophy after P8 [12, 13]. Together, this suggests loss of *STAMBP* function is an underlying mechanism in microcephaly and its progression in MICCAP syndrome. Ubiquitinated protein aggregation in neurons is linked to neurodegenerative disorders, such as Alzheimer's disease, frontotemporal dementia, and amyotrophic lateral sclerosis. It has been reported that *STAMBP*-deficient mice showed ubiquitinated aggregates of p62 and TDP-43 prior to neurodegeneration in the brain [12]. In addition to regulating aggregate formation through ubiquitin

binding, p62 is degraded in autolysosome, which is a single membrane organelle that forms in the course of autophagy upon fusion of autophagosomes and lysosomes [14]. Based on these reports, *STAMBP* may be essential to autophagic clearance of aggregated proteins by promoting the autophagosome–lysosome fusion [12].

Our analysis of phosphorylated S6 expression was inconsistent with a previous study that showed LCLs from patients with *STAMBP* alterations had higher amounts of pS6 compared to controls, indicating constitutive activation of the PI3K–AKT–mTOR pathway under starved conditions [1]. In this case patient, the reduction of pS6 in patient-derived cells under starved conditions was similar to that of control cells, indicating that our patient did not demonstrate starvation-insensitive activation of pS6. While we did not test the function of RAS–MAPK signaling, as activation of the RAS–MAPK pathway activates the PI3K–AKT–mTOR pathway through suppression of the TSC1/2 complex, it is unlikely that constitutive activation of the RAS–MAPK pathway underlies the pathomechanism in our patient. Other mechanisms however, such as dysfunction of autophagy, may be the major contributor to the pathomechanism in our patient.

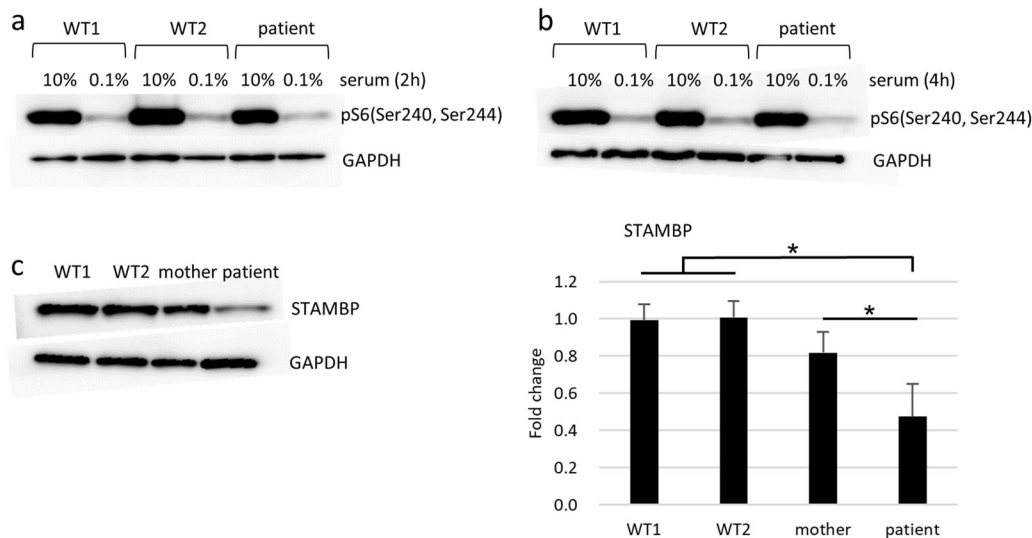


**Fig. 4** Protein expression analysis of PI3K–AKT–mTOR pathway and STAMBP. **a, b** Serum starvation of WT and patient-derived LCLs for 2 h (**a**) and 4 h (**b**) reduced phosphorylation of Ser240 and Ser244 residues of S6 protein in LCLs as well as WT LCLs. Representative western blots are shown. **c** Immunoblot analysis of STAMBP protein from patient-derived LCLs and the mother. The homozygous mutant

patient showed markedly decreased the expression levels, while the heterozygous mutant mother showed mildly decreased the expression levels although this was not statistically significant. Representative images and quantitative analysis of band intensities are shown. PS6 and STAMBP intensities were standardized by GAPDH intensities and compared using a two-tailed Student's *t* test; \**p* < 0.05

Capillary malformations, also known as port-wine stains, are cutaneous vascular abnormalities seen in congenital genetic syndromes associated with RAS–MAPK pathway dysregulation, also known as “RASopathies” [15]. Signaling by the RAS–MAPK and PI3K–AKT–mTOR pathways regulate fundamental cellular processes, including cell growth, cell-cycle progression, and differentiation. Although McDonnell et al. [1] postulated that the RAS pathway may be responsible for capillary malformations, our results suggest that other mechanisms may contribute to the phenotype.

The clinical features of the case patient are somewhat mild compared to those previously reported with MICCAP, in which almost all had congenital microcephaly, hypoplastic distal phalanges, and early-onset intractable seizures. Our patient had a normal head circumference at birth, no hypoplastic distal phalanges, and did not develop epilepsy until 7 months of age. Our patient, however, does share some clinical features with previously reported MICCAP, such as cortical atrophy, intractable epilepsy, and profound developmental delay. The mild clinical presentation in our patient may be explained by the minimal involvement of the RAS–MAPK and PI3K–AKT–mTOR pathways. Furthermore, mild microcephaly might explain the relatively slow-onset epilepsy as volume reduction has been associated with seizure frequency and epilepsy duration [16].

**Acknowledgements** This study was supported in part by a grant for Research on Applying Health Technology from the Ministry of Health, Labour and Welfare of Japan to F.M., N.O., M.K., M.Y., Y.K., K.K., and S.S.

## Compliance with ethical standards

**Conflict of interest** The authors declare that they have no conflict of interest.

## References

- McDonnell LM, Mirzaa GM, Alcantara D, Schwartzentruber J, Carter MT, Lee LJ, et al. Mutations in STAMBP, encoding a deubiquitinating enzyme, cause microcephaly-capillary malformation syndrome. *Nat Genet.* 2013;45:556–62.
- Carter MT, Geraghty MT, De La Cruz L, Reichard RR, Boccuto L, Schwartz CE, et al. A new syndrome with multiple capillary malformations, intractable seizures, and brain and limb anomalies. *Am J Med Genet A.* 2011;155:301–6.
- Mirzaa GM, Paciorkowski AR, Smyser CD, Willing MC, Lind AC, Dobyns WB. The microcephaly-capillary malformation syndrome. *Am J Med Genet A.* 2011;155:2080–7.
- Isidor B, Barbarot S, Beneteau C, Le Caignec C, David A. Multiple capillary skin malformations, epilepsy, microcephaly, mental retardation, hypoplasia of the distal phalanges: report of a new case and further delineation of a new syndrome. *Am J Med Genet A.* 2011;155:1458–60.
- Faqeih EA, Bastaki L, Rosti RO, Spencer EG, Zada AP, Saleh MA, et al. Novel STAMBP mutation and additional findings in an Arabic family. *Am J Med Genet A.* 2015;167:805–9.
- Pavlovic M, Neubauer D, Al Tawari A, Heberle LC. The microcephaly-capillary malformation syndrome in two brothers with novel clinical features. *Pediatr Neurol.* 2014;51:560–5.
- Naseer MI, Sogaty S, Rasool M, Chaudhary AG, Abutalib YA, Walker S, et al. Microcephaly-capillary malformation syndrome: brothers with a homozygous STAMBP mutation, uncovered by exome sequencing. *Am J Med Genet A.* 2016;170:3018–22.
- Negishi Y, Miya F, Hattori A, Mizuno K, Hori I, Ando N, et al. Truncating mutation in NFIA causes brain malformation and urinary tract defects. *Hum Genome Var.* 2015;2:15007.

9. Purcell S, Neale B, Todd-Brown K, Thomas L, Ferreira MA, Bender D, et al. PLINK: a tool set for whole-genome association and population-based linkage analyses. *Am J Hum Genet.* 2007;81:559–75.
10. Sierra MI, Wright MH, Nash PD. AMSH interacts with ESCRT-0 to regulate the stability and trafficking of CXCR4. *J Biol Chem.* 2010;285:13990–4004.
11. Tanaka N, Kaneko K, Asao H, Kasai H, Endo Y, Fujita T, et al. Possible involvement of a novel STAM-associated molecule “AMSH” in intracellular signal transduction mediated by cytokines. *J Biol Chem.* 1999;274:19129–35.
12. Suzuki S, Tamai K, Watanabe M, Kyuuma M, Ono M, Sugamura K, et al. AMSH is required to degrade ubiquitinated proteins in the central nervous system. *Biochem Biophys Res Commun.* 2011;408:582–8.
13. Ishii N, Owada Y, Yamada M, Miura S, Murata K, Asao H, et al. Loss of neurons in the hippocampus and cerebral cortex of AMSH-deficient mice. *Mol Cell Biol.* 2001;21:8626–37.
14. Pankiv S, Clausen TH, Lamark T, Brech A, Bruun JA, Outzen H, et al. p62/SQSTM1 binds directly to Atg8/LC3 to facilitate degradation of ubiquitinated protein aggregates by autophagy. *J Biol Chem.* 2007;282:24131–45.
15. Rauen KA. The RASopathies. *Annu Rev Genomics Hum Genet.* 2013;14:355–69.
16. Lawson JA, Vogrin S, Bleasel AF, Cook MJ, Burns L, McAnally L, et al. Predictors of hippocampal, cerebral, and cerebellar volume reduction in childhood epilepsy. *Epilepsia.* 2000;41:1540–5.